UCRL-JC-127867
PREPRINT

Insensitive HE EOS

F.H. Ree
J. Viecelli
M. van Thiel

This paper was prepared for submittal to the
11th Biennial Nuclear Explosives Design Physics Conference
Livermore, CA
October 20-24, 1997

December 1997

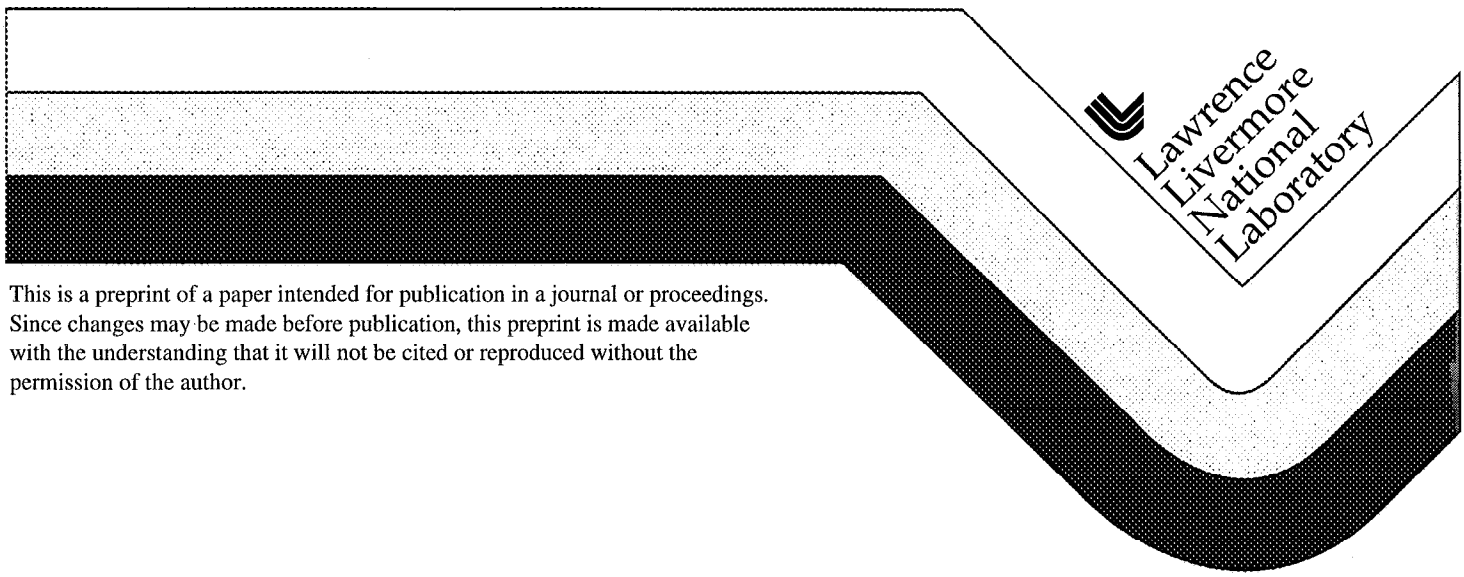

Insensitive HE EOS

F. H. Ree, J. Viecelli, and M. van Thiel
Lawrence Livermore National Laboratory

A typical insensitive high explosive such as LX-17 has a large carbon-content and produces hydrogen fluoride (HF) as a detonation product. It is also characterized by slow energy release as indicated by a large curvature of the detonation front. We analyze these new physics issues which are needed to predict the performance of a insensitive high explosive. (U)

Introduction

Present production hydro codes incorporate an empirical equation-of-state (EOS) that is matched to cylinder shots or hydros. These EOSs are based only on a single track in phase space. Our task is the generation of reliable multi-track high explosives (HE) EOS data (overdriven detonation, reshock, adiabats, etc.) with enhanced predictive accuracy for SBSS applications. For this reason, we have put a considerable effort to develop the CHemical Equilibrium (CHEQ) code (Ree, 1984) by upgrading its scientific content and computational versatility. The CHEQ code is unique in its use of reliable statistical mechanical theories, interaction potentials, and its ability to handle multi-phase fluid mixtures. It appears from a number of calculations that the CHEQ EOS for HE, such as LX-14, gave almost uniformly similar and rather good results. A similar assessment for a more insensitive high explosive (IHE) is now under way.

An IHE with high safety and high performance is preferred over a sensitive HE. The former differs from the latter not only in initiation characteristics but also in detonation characteristics. IHE (e.g., LX-17) is characterized by (i) large carbon-content, (ii) presence of HF as a detonation product, and (iii) slow energy release as indicated by a large curvature of the detonation front and a large diameter-dependence of the detonation velocity. We are investigating each of these three aspects over an extended density and temperature range. This is done by investigating: (a) carbon kinetics, (b) the HF-HF intermolecular potential and those between HF and other detonation products, (c) the effect of F-chemistry on supercritical fluid phase change present in mixtures containing H_2O and N_2, and (d) an incomplete burn of HE. This paper describes the relevance of the new physics issues mentioned above to the performance of IHE.

Carbon kinetics

In the gas phase reactions are fast in comparison to hydrodynamic time scales of interest. In contrast, reactions involving solid or liquid products are slow, i.e., comparable to hydrodynamics time or even longer. In IHE detonations, carbon residues are a major solid product. Hence, it is important to consider the kinetics of the carbon condensation processes (Van Thiel and Ree, 1987) and their effects on IHE EOS. As will be shown below, it has a significant effect on the computed detonation properties of carbon-rich HEs.

Carbon condensation can involve two main steps. The first step is concerned with coagulation of atomic carbon from gaseous detonation products through diffusion to build up gradually larger carbon clusters. Their growth kinetics have been examined by Johnson and Shaw (1987) using the Smoluchowski equations,

$$dc_k/dt = \sum_{i+j=k} k_{ij} c_i c_j - 2c_k \sum_j k_{jk} c_j, \qquad (1)$$

where k_{ij} describes the rate constant for coagulation of cluster i (with i carbon atoms and concentration c_i) with clusters of size j with concentration c_j. We use Johnson and Shaw's approximation for k_{ij} which provides a simple analytic expression for c_i. The surface contribution ΔG_k to the Gibbs free energy can be obtained by averaging the surface energy per particle, $\Delta E_k \approx A/k^{1/3}$, over c_k. We have implemented the above carbon clustering kinetics in the CHEQ code to account for a time-dependent surface correction to the Gibbs free energy.

Figure 1 illustrates the effect of the carbon phase change on detonation velocity of TNT with different initial densities. The lower curve is based on the assumption of thermodynamic equilibrium. This is the case if the pressure and temperature in the detonation wave can achieve equilibration very fast. However, the actual carbon particles that are produced within the time scale of detonation experiments are very small. Hence, thermodynamic properties of these small carbon clusters are different from that of bulk carbon. We expect that, depending on the size of carbon particles, the transformation of graphitic carbon to the diamond-like form will occur at a different pressure and temperature.

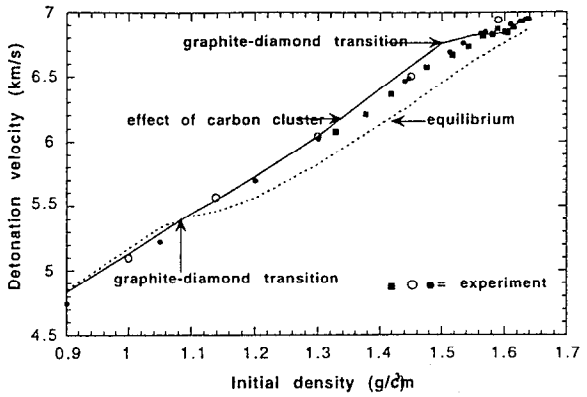

Figure 1. Detonation velocity vs. initial density of TNT. See van Thiel and Ree (1981) for experimental references.

The upper curve is obtained with the 'nonequilibrium' CHEQ code (which contains the carbon cluster diffusion described above) using reasonable values for the surface energy constant of diamond and graphitic clusters. The calculation was done at 150 ns behind the detonation front. This time interval can be regarded as a typical reaction zone thickness of the detonation front for TNT. By adjusting the diamond surface energy constant A and using the experimental value of A for graphite, we can raise the transition pressure (hence, the detonation velocity) and, thereby, make the theoretical prediction agree closer with experimental data referenced in our earlier similar but simpler calculation (Van Thiel and Ree, 1987) which uses a parameter describing the formation energy of the diamond particles to match the experimental data. The present model can also reliably predict the overdriven shock wave data and the detonation velocity data with various initial densities. The nonequilibrium CHEQ code described above is expected to provide an important input to the understanding of the performance of carbon-rich explosives.

As mentioned earlier, clusters formed during the first step are small. Consideration of the surface energy favors these clusters to be graphitic with sp^2-like bonding as opposed to diamond with sp^3-like bonding. As the clusters grow larger, surface contributions to thermodynamic properties becomes less important and diamond-like clusters become energetically favored. However, a reaction barrier between the two phases will kinetically limit the graphitic-to-diamond transformation process. This second kinetics step needs to be investigated, as there is no a priori reason to favor the first (i.e., diffusion) step over the second. We are presently investigating this aspect (Ree et al., 1997) using the bond order potential developed by Brenner (1990). The Brenner potential predicts correct structures for all the common hybridization states (sp, sp^2, and sp^3) of carbon and allows for the breaking and formation of covalent carbon bonds. We tested the applicability of the Brenner potential by computing the diamond melting line, the graphite melting line, and the local structure of the liquid phase by molecular dynamics simulations.

This information is displayed in Fig. 2 along with the phase diagram based on available experimental and theoretical data. The two diamond melting lines cover uncertainties of the melting line estimated by van Thiel and Ree (1992). Notice that the simulation study predicts a melting line which is consistent with the best available data. Our simulations show that the structure of the liquid at high density is mostly four-fold coordinated or sp^3-like and at low density it is two-fold coordination or sp-like. So we observe a change in the local structure with density. The Brenner potential as presently developed has neglected the long-range van der Waals forces which may be important for holding graphitic sheets together. Possible improvement of the Brenner potential in this connection is under consideration.

The height of the reaction barrier for the graphite to diamond transition and the heat of formation of carbon clusters are needed to study the graphite-to-diamond transformation kinetics. Energies along model reaction paths on the hypersurface describing the convergence from sp^2 to sp^3 bonding were also determined using the first principles and semiempirical molecular orbital methods (Ree et al., 1997). The reaction path was defined by linear interpolation between the reactant and product structures. While the reaction coordinate does not necessarily correspond to the minimum energy path for the phase transformation, it allows us to make a consistent comparison of the predictions of the various electronic structure methods. These calculations predict

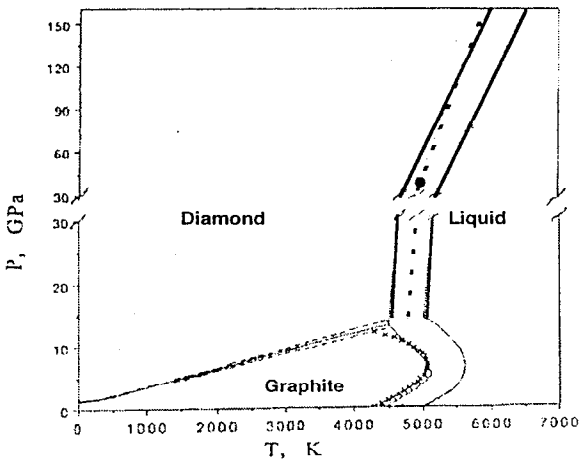

Figure 2. Phase diagram of carbon: solid circle = melting point based on the Brenner potential; dashed line = melting line derived from the solid circle. It lies within the range of uncertainties of the melting line as indicated by two solid lines (van Thiel and Ree, 1992).

similar activation energies of 0.32 eV/atom to 0.4 eV/atom. These are in agreement with the calculated bulk activation energies for the graphite-diamond phase transformation based on the local density approximation (Fahy et al., 1987).

Intermolecular potentials of HF

A typical IHE such as LX-17 produces hydrogen fluoride (HF). Hence, the performance prediction of an IHE requires information on intermolecular potentials related to HF. However, experimental data (e.g., shock wave) on HF relevant to the present work are almost non-existent because of its corrosive nature. Furthermore, HF is a strongly hydrogen bonding system, which, in spite of its simplicity, makes predicting its intermolecular potential difficult. We describe below our attempt to obtain the HF pair potentials based on available data.

We use the structure of condensed HF at low temperatures as a guide. HF molecules have a hydrogen bond strength of about 0.3 eV and form chain- and ring-clusters in the gas and liquid phases. The crystals structure of HF is orthorhombic with space group C_{2v}^{12}. It consists of zigzag hydrogen bonded F-F chains that are parallel to the [100] plane. The F-F bond distance in the chain is 2.49 Å at 148 K and the nearest neighbor interchain distances are 3.12 to 3.20 Å.

Figure 3 shows these inter- and intra-chain distances of the crystal structure and also several HF-HF potentials (with $\varepsilon = \varepsilon_0$) based on quantum mechanical and semiempirical calculations and represented by an exponential-6 potential,

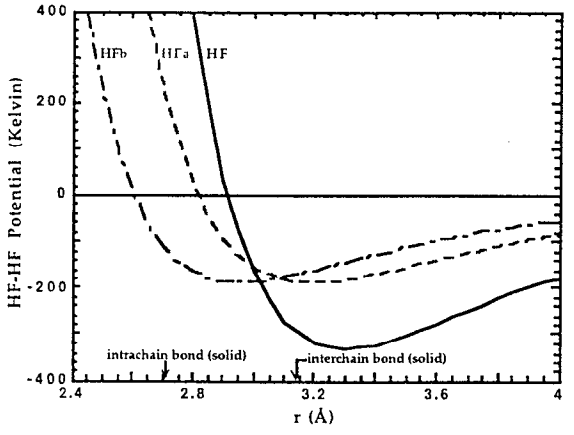

Figure 3. Pair potentials for HF used in the analysis of fluorine containing explosive formulations. See the text for parameters for these potentials. Arrows indicate intrachain (= strongly H-bonded) and interchain (= weakly H-bonded) F-F distances in the crystal.

$$\phi(r) = \frac{e}{a-6}\{\, 6\exp[\alpha(1 - r/r^*)] - \alpha(r^*/r)^6 \,\}, \quad (2)$$

where the well depth ε is here temperature dependent and has the high temperature form,

$$\varepsilon = \varepsilon_0(1 + \lambda/T), \quad (3)$$

which describes the increasingly attractive character of the interaction as the temperature decreases. Note that this term is a high temperature correction and becomes less reliable at $T < \lambda$.

Our first attempt at determining the HF-HF pair potential is indicated as "HF" in the figure. Its repulsive range was too large to match detonation properties of five high explosives (Van Thiel and Ree, 1995): FEFO($C_5H_6N_4O_{10}F_2$), FM1($C_{1.906}H_{2.872}N_{1.265}O_{3.164}F_{0.308}$), PF($C_6H_2N_3O_6F_1$), LX-17($C_{2.295}H_{2.186}N_{2.150}O_{2.150}F_{0.2}$), and 1,2DP($C_3H_6N_2F_2$).

This potential has a minimum value at r* (= 3.30 Å) > r_e = 3.12 Å (= the smallest interchain F-F distance). Another potential, with r* (= 2.95 Å) < r_e, labeled HFb in Fig. 3, was obtained using the D_{CJ} of 1,2DP. Since it gave inconsistent detonation velocities of the other explosives it has been rejected. The best available potential (labeled HFa) was obtained by spherical averaging the *ab initio* data of Barton and Howard weighted by a Boltzman factor (Ree and Calef, 1990). Numerical values of the potential HFa and HFb are:

HFa:
ε/k = 188.6K, r* = 3.19Å, α = 13.01, λ = 368.6K,

HFb:
ε/k = 188.6K, r* = 2.95Å, α = 13.01, λ = 368.6K,

Note that its potential minimum (r* = 3.19 Å) is close to r_e. The differences in the calculated detonation velocities (D_{CJ}) between the HFa and HFb potentials are about 2.5 % for FEFO and LX-04. These are significant differences. The present work shows that accurate knowledge of the HF interaction potential is critical to the HE performance prediction.

In this work, the HFa potential was used to fine tune the unlike-pair interactions between HF and other detonation products such as CO_2, H_2O, CO, and NH_3 by using the generalized Lorentz-Berthelot rule (Ree, 1984),

$$\varepsilon_{ij} = k_{ij}\sqrt{\varepsilon_{ii}\varepsilon_{jj}},\ r_{ij}^* = \frac{1}{2}l_{ij}(r_{ii}^* + r_{jj}^*),$$
$$\alpha_{ij} = m_{ij}\sqrt{\alpha_{ii}\alpha_{jj}}, \quad (4)$$

with constants appropriate for the HFa potential. The refinements (k_{ij}, l_{ij}, and m_{ij}) of the unlike pair ($i \neq j$)

interaction parameters, originally set equal to 1, are done using D_{CJ} data of FEFO, LX-04($C_{1.55}H_{2.58}N_{2.30}O_{2.30}F_{0.52}$), and 1,2DP.

We should emphasize that the overall determination of the interactions is sensitive to the accuracy and completeness of the experimental data and also to the details of the carbon cluster model, since an appreciable fraction of the product composition is carbon. The above HF interaction analysis was done with an empirically adjusted carbon cluster equation of state calibrated to the performance of TNT($C_7H_6N_3O_5$) (Van Thiel, et al., 1995). Table 1 shows the resulting parameter set, Set A.

More recently two changes were introduced in the analysis. First, the carbon cluster model was changed to one explicitly allowing for the growth of clusters by diffusion discussed earlier. Second, comparison of the original CHEQ LX-04 CJ adiabat with a new LX-04 Jones-Wilkins-Lee (JWL) EOS by Bradley (1997),

$$P = A(1-\frac{\omega}{R_1V})\exp(R_1V) + B(1-\frac{\omega}{R_2V})\exp(R_2V)+\frac{\omega E}{V}, \quad (5)$$

with A = 6.310, B= 0.1932, R_1 = 4.25, R_2 = 1.45 ,and ω = 0.25 showed the CHEQ adiabat pressure falling 5 to 10% below the JWL in the region below the CJ point. This was done by adjusting the HF potentials to raise the pressure on the LX-04 CJ adiabat based on Set A, in the region below the CJ point, so that it would be in better agreement with the new JWL, subject to the constraint that the pair potential adjustments should cause the theoretical D_{CJ} to agree with the experimental detonation velocities for FEFO and LX-04. The parameter set (Set B) resulting from these adjustments noticeably alters the CHEQ LX-04 adiabat above the CJ point but not below the CJ point.

Table 1. Lorentz-Berthelot correction factors, Eq. (3), for unlike-pair interaction constants.

Correction factor	Set A		
	k	*l*	*m*
H_2O - HF	1.0	1.101	1.0
CO_2 - HF	1.0	0.841	1.0
CO - HF	1.0	1.0	1.0
Correction factors	**Set B**		
	k	*l*	*m*
H_2O - HF	1.0	0.976	1.0
CO_2 - HF	1.0	1.095	1.0
CO - HF	1.0	1.080	1.0

Table 1 shows numerical values for parameter sets A. In Set A we chose the constants for the CO-HF interaction to be *k/l/m* = 1/1/1, since the effect on the detonation pressure was too small to offer a good test. Table 2 shows the resulting the CJ pressures (P_{CJ}) and detonation velocities. In addition, the effect of using the HFb potential, instead of HFa, is shown. The importance of a careful self-consistent approach in determining the effective potentials is hereby underscored.

Table 2. Effects of correction factors (given in Table 1) on D_{CJ} and P_{CJ}.

Pot-ential	Corr. factor	FEFO D_{CJ} km/s	FEFO P_{CJ} GPa
HFa	Set A	7.40	24.3
HFa	Set B	7.51	24.9
HFb	Set B	7.70	26.7
Experiment		7.50	25.0

Pot-ential	Corr. factor	LX-0 4 D_{CJ} km/s	LX-0 4 P_{CJ} GPa
HFa	Set A	8.65	31.7
HFa	Set B	8.45	32.8
HFb	Set B	8.67	35.0
Experiment		8.46	35.0

Effects of fluorine chemistry on supercritical fluid phase changes

Currently available studies on supercritical fluid phase separations are limited to mixtures of chemically nonreactive species. These are not directly relevant to describe the postdetonation products of HEs which contain chemically reactive mixtures such as CO, CO_2, H_2O, N_2, etc. In addition, our earlier statistical mechanical calculations revealed that post-detonation mixtures containing C, N, H, O atoms separate into an N_2-rich and an N_2-poor fluid phases near or above the CJ point. A binder such as Kel-F or viton A used in the formulation of an IHE contains F atoms in addition to C, N, H, O atoms. They react with H or C atoms to produce HF and CF_4. Here we need to be concerned with a possible influence of chemical reactions involving these additional species on the N_2-rich and an N_2-poor phases. Such calculations are carried out in this work for an IHE (LX-17) which has the Kel-F binder and a more sensitive HE (LX-04) with viton A binder.

Figure 4 shows two Hugoniots of LX-17 based on CHEQ, assuming the HE to burn 100% and 96.5%, respectively. Both calculations use the HFa set for the HF-HF potential and Set A (in Table 1) for interactions between HF and other detonation products. The reason for the two calculations will be elaborated in the next section. We will focus here the Hugoniot with 96.5% burn, which shows a 'kink' near 50 GPa. This is attributed to the fluorine chemistry which drastically complicates the previously known phase separation between the N_2-rich and N_2-poor phases. Namely, up to about 50 GPa, F atoms prefer to form HF molecules and occur in the N_2-poor phase, which contains mostly H_2O molecules. This is attributed to the fact that HF and H_2O are the two strongest hydrogen-bonding molecules and that they prefer to associate with each other. However, if the pressure and temperature exceeds this range, F atoms tend to form CF_4 molecules in the N_2-rich phase. Namely, a high pressure forces F atoms to be more compact so that the free energy of the mixture can be lowered (Le Chaterlier's principle).

In Fig. 5 we elaborate this shift in fluorine chemistry by comparing the mole fractions (= moles/total number of moles in a given phase) of N_2, H_2O, HF, and CF_4 along the 0.5-eV isotherm of LX-04. We note that the addition of F atoms produces three different characteristics to the N_2-rich and an N_2-poor phases at different levels of pressures, $P_1 < P_2 < P_3$. First, within a small pressure interval (P_1, P_2) indicated by a mid-arrow (above x-axis at 30 GPa) in Fig. 5, fluid mixtures separate into Phases α and β, in which Phase α is rich in HF and Phase β is rich in both N_2 and H_2O. At the next pressure interval, $P_2 < P < P_3$, H_2O molecules in Phase β gradually change their phase preference to Phase α so that they can be close to

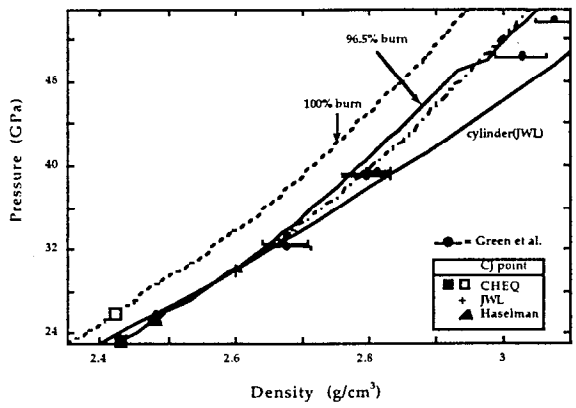

Figure 4. Hugoniots of LX-17 using the HFa parameters for the HF-HF potential and Set A for unlike-pair potentials: solid line = 100% burn and dashed line = 96.5%. Also shown are: experimental data (Green et al., 1985), the JWL fit to cylinder tests, and Haselman's work (1987).

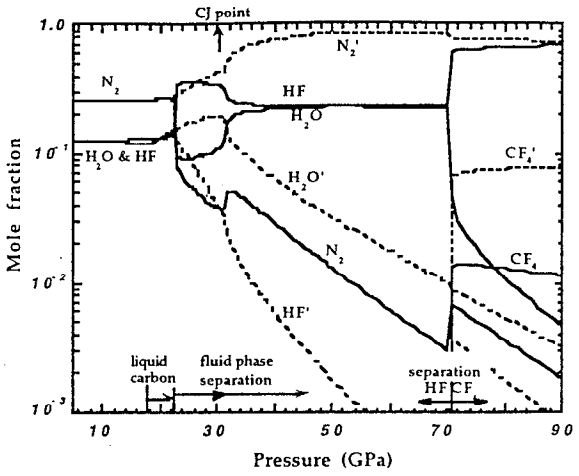

Figure 5. Mole fractions of detonation products along the 0.5 eV isotherm of LX-04, based on the HFa parameters for the HF-HF potential and Set A for unlike-pair potentials: solid line = Phase α and dashed line = Phase β.

similar hydrogen-bonding molecules, HF. At the third pressure interval, $P > P_3$, HF molecules in Phase α become thermodynamically less stable with respect to formation of CF_4 molecules, which prefer to be in Phase β, associated with the N_2-rich phase. This last phase separation occurs at pressure P_3 which is well above P_1 and is abrupt in thermodynamic sense. Examination of Fig. 5 shows that this phase separation involves the formation of diamond through a chemical reaction,

$$2CO(\beta) + 4HF(\alpha) \longrightarrow CF_4(\beta) + 2H_2O(\alpha) + C(\text{diamond}).$$

Figure 4 shows that the pressure P_3 at the third phase boundary can be as low as about 10 GPa to 20 GPa at 1000 K. These ranges of pressure and temperature should be accessible to present-day experimental high-pressure techniques; hence, it will be worthwhile to experimentally confirm the prediction made here. However, it should be noted that this shift in fluorine chemistry is extremely delicate and sensitive to unlike pair potentials between HF and other species. For example, if Set B is used instead of Set A, the shift in fluorine chemistry, $HF(\alpha) \longrightarrow CF_4(\beta)$, coincides with the pressure (P_1) where the N_2-rich fluid phase separation occurs at first and no additional change in the character of the fluid phase separation is predicted at higher pressures.

Incomplete burn of IHE

Another important physics issue is an indication that an IHE tends to burn slowly or incompletely. Assuming equilibrium behind the detonation wave, the

detonation temperature (T_{LX17}) of LX-17 is about 3100 K, while LX-14 detonates at an equilibrium temperature T_{LX14} = 4100 K. One can make a crude estimate on the chemical reactions involving the detonation of LX-14 and LX-17 by assuming the rate equation,

$$R = \eta\, e^{-T^*/T}, \qquad (6)$$

where $\eta = \kappa\, kT/h$ and κ = transmission coefficient ≈ 0.5.

For TNT, T_{TNT} = 3800 K and $\eta = 6.10^{13}$. The rate for detonation is R = 1 ns^{-1} which is consistent to describe the energy profile of the TNT detonation front. Hence, the energy of activation is T* ≈ 39,000 K. Assuming that T* is approximately the same for LX–14 and LX-17 (Sheffield et al., 1984), we estimate that

$$R_{LX14}/R_{LX17} = \exp[-T^*(1/T_{LX14} - 1/T_{LX17})] = 104,$$

indicating that, behind the detonation front, LX-17 burns about 100-times slower than LX-17.

This physical picture is also consistent with the observation on another TATB formulation, i.e., EDC35 containing 5% Kel-F (Hutchinson, et al., 1989). This HE shows an increase of 2.7% in D_{CJ} when the diameter of the charge was increased from 12.7 mm to 127 mm. Furthermore, the charge fails to detonate for densities greater than 1.93 g/cm^3, due to the lower detonation temperature in the relatively void free charge.

Figure 4 further illustrates the effects of a slow burn front. It compares the CHEQ Hugoniot of LX-17 with the overdriven shock experiments of Green et al. (1985), cylinder tests, and a recent work by Haselman (1997) which agrees with the overdriven shock wave data. The theoretical CHEQ results are clearly much stiffer than the others. A reduction in the amount of burn allowed in the calculation brings the theory closer to experiment. It implies that effectively about 3% of the TATB in the formulation has not fully reacted.

Not shown are the CJ expansion adiabat below the CJ point. A 3.5% reduction in the amount of the HE burn also offers good agreement with Haselman's analysis below 11 GPa. Above that point but below the CJ point, there are two issues which complicate the theoretical analysis; i.e., question of cluster size and the reverse transformation rate from diamond-like clusters to graphitic clusters.

At low pressure the graphitic state is more stable, while at higher pressure diamond-like clusters form. The carbon cluster growth model discussed earlier in this work indicates that a reduction in cluster size shifts the pressure at which the clusters transform to a diamond-like state to higher pressure. Smaller clusters imply a lower diamond stability and a higher transformation pressure. Therefore, the slow or incomplete burn may be related to an effective small carbon cluster size, which can capture other molecule or atoms (e.g., O, H, OH, or NO) to their surface. These clusters, therefore, look like large molecules that are intermediate burn products. Furthermore, they are released to the gas phase, providing additional kinetic energy to the detonation.

Second, as the pressure decreases along the adiabat, carbon clusters in the mixture system need to undergo a reverse transformation from diamond to graphite clusters. Along the expansion adiabat, this transformation which is likely in martensitic in nature may be much slower in comparison to the hydrodynamic time scale than the situation at the CJ point. The degree to which both kinetic processes, associated with the cluster coagulation and the martensitic transformation, go to completion as well as a possible coupling between the two again depend on temperature and pressure. Current work (in molecular dynamics and first principles calculations) is designed to improve the model in this direction.

Acknowledgment

This work was done under the auspices of the U.S. Department of Energy by the Lawrence Livermore National Laboratory under contract number W-7405-ENG-48. We thank Dr. Yim Lee for his contributions to the EOS of LX-04 and Drs. Nicholas Winter and James Glosli for discussing their work on carbon discussed in this paper.

References

Ree, F. H., *J. Chem. Phys.*, **81**, 1251 (1984).

Van Thiel, M. and Ree, F. H., *J. Appl. Phys.*, **62**, 1761 (1987); also see references quoted therein.

Shaw, M. S. and Johnson, J. D., *J. Appl. Phys.*, **62**, 2080 (1987).

Ree, F. H. Glosli, J. and Winter, N., "Equilibrium and nonequilibrium properties of bulk and nanosize clusters of carbon," *Special issues of The Review of High Pressure Science and Technology*, Vol. 6, 1997, The Japan Society of High Pressure Science and Technology, Kyoto, Japan. (to be published.)

Brenner, D. W., *Phys. Rev.*, **B42**, 9458 (1990).

Van Thiel, M., and Ree, F. H., *High Pressure Research*, **10**, 607 (1992); also see references quoted therein.

Fahy, S., Louie, S. G., and Cohen, M. L., *Phys. Rev.*, **B35**, 7623 (1987); also see references quoted therein.

Van Thiel, M., Ree, F. H., and Haselman, L. C., "Accurate Determination of Pair Potentials for a $C_wH_xN_yO_z$ System of Molecules: A Semiempirical Method," Report UCRL-ID-120096 (Lawrence Livermore Laboratory, 1995).

Ree, F. H., and Calef, D. F., "Theoretical Hugoniot of Liquid Hydrogen Fluoride," in *Shock Compression of Condensed Matter-1989*, Eds. S. C. Schmidt, J. N. Johnson, and L. W. Davison (Elsevier Science, NY, 1990) p. 91.

Bradley, K. private communication (1997).
Sheffield, S. A., and Bloomquist, D. D., J. Chem. Phys. **80**, 3831 (1984)15.
Hutchinson, C. D., Foan, G. C. W., Lawn, H. R., and Jones, A. G., "Initiation and detonation properties of the insensitive high explosive TATB-Kel-F 800 95/5," in *Proc. Ninth Symposium (International) on Detonation*, Portland, OR (1989), OCNR 113291-7 Vol I, (Office of the Naval Research, Arlington VA 22217-5000, 1989) p. 123.
Green, L., Lee, E., Mitchell, A., and Tarver, C., "The supra compression of LX-04, LX-17, PBX-9404, and RX-26-AF and the equations of state of the detonation products," in *Proc. Eighth Symposium (International) on Detonation*, Albuquerque, NM July 1985, NSWC MP 86-194, (Naval Surface Weapons Center, White Oak, Silver Spring, MD 20903-5000, 1986) p. 587.
Haselman, L., private communication (1997).

Technical Information Department • **Lawrence Livermore National Laboratory**
University of California • Livermore, California 94551